Title

In VivoFluorescence Detection of Ovarian Cancer in the NuTu-19 Epithelial Ovarian Cancer Animal Model Using 5-Aminolevulinic Acid (ALA)

Journal

Gynecologic Oncology, 66(1)

ISSN

0090-8258

Authors

Major, Attila L

Rose, G Scott

Chapman, Curtis F

et al.

Publication Date

1997-07-01

DOI

10.1006/gyno.1996.4502

GYNECOLOGIC ONCOLOGY **66,** 122–132 (1996)
ARTICLE NO. GO964502

In Vivo Fluorescence Detection of Ovarian Cancer in the NuTu-19 Epithelial Ovarian Cancer Animal Model Using 5-Aminolevulinic Acid (ALA)

Attila L. Major,*,†,[1] G. Scott Rose,‡ Curtis F. Chapman,* John C. Hiserodt,§ Bruce J. Tromberg,* Tatiana B. Krasieva,* Yona Tadir,* Urs Haller,† Philip J. DiSaia,‡ and Michael W. Berns*

**Beckman Laser Institute, University of California, Irvine, Irvine, California 92715; †Department of Obstetrics and Gynecology, University Hospital, Zurich, Switzerland; and Division of ‡Gynecologic Oncology and §Pathology, University of California, Irvine, UCI Medical Center, Orange, California 92668*

Received April 5, 1996

The purpose of this study was to determine whether *in vivo* **fluorescence detection of protoporphyrin IX (PpIX) could be used to identify intraperitoneal micrometastases of epithelial ovarian carcinoma after application of 5-aminolevulinic acid (ALA). ALA was applied intraperitoneal at different concentrations (25, 50, and 100 mg/kg) and iv (100 mg/kg) to immunocompetent Fischer 344 rats bearing a syngeneic epithelial ovarian carcinoma. At different time intervals after ALA administration (1.5, 3, and 6 hr) the peritoneal cavity was illuminated with ultraviolet (uv) light.** *In vivo* **fluorescence of PpIX initially was determined by direct visualization. Subsequently** *ex vivo* **measurements were made with a slow-scan, thermoelectrically cooled CCD camera. Red** *in vivo* **fluorescence was observed in ovarian micrometastases smaller than 0.5 mm in 100% of the ALA-administered animals independent of time interval, drug concentration, or route of administration. The intensity of the fluorescence was concentration dependent as strong fluorescence was consistently found only above 25 mg/kg ALA.** *Ex vivo* **tumor to peritoneum fluorescence yield peaked 3 hr after administration of a 100 mg/kg intraperitoneal dose. Direct visualization of** *in vivo* **fluorescence after ALA application may improve the detection of intraperitoneal ovarian cancer micrometastases.**

INTRODUCTION

Ovarian carcinoma is the fourth most frequent cause of cancer-related death in women in the United States [1]. Many patients with advanced disease (stage III and IV) initially respond to standard therapies, as evidenced by negative second-look laparotomies. Unfortunately, up to 50% of these cases will recur and inevitably result in death [2]. As a result, it is necessary to develop improved diagnostic and therapeutic methods which offer the possibility of early detection and more effective eradication of the disease. The use of photomedicine techniques such as photodynamic therapy (PDT) and *in vivo* fluorescence detection using lesion localizing photosensitizers have been suggested as novel interventions in cancer patients [3, 4].

While there has been great interest in the use of PDT in cancer treatment, there have been no reports of its use as a diagnostic aid in ovarian cancer second-look laparotomy procedures. Second-look procedures have not been shown to have a positive effect on patient survival and are currently only recommended for patients on research protocols or in settings where salvage therapies are available [5, 6]. In addition, the false-negative rate of this procedure has been shown to be exceedingly high. As many as 50% of patients with negative second-look laparotomies will experience recurring disease within 5 years and will ultimately succumb to their disease [7]. Even the most thorough reexploration, employing multiple pelvic and upper abdominal washings and biopsies, does not necessarily result in sensitive, reliable diagnosis of microscopic residual disease [2]. Therefore, a procedure which is minimally invasive, has few side effects, and could assist in the diagnosis of microscopic residual disease would be of great value.

Exogenously applied 5-aminolevulinic acid (ALA) results in endogenous production of the potent, fluorescent photosensitizer protoporphyrin IX (PpIX) [8]. ALA, by itself, is not a photosensitizing agent, but is the precursor of PpIX in the biosynthetic pathway of heme. Physiologically, the production of heme regulates the synthesis of ALA via a mechanism of negative feedback. Administration of exogenous ALA bypasses this mechanism and induces accumulation of PpIX in certain cells [8]. ALA-induced PpIX synthe-

[1] To whom correspondence should be addressed at Beckman Laser Institute and Medical Clinic, 1002 Health Sciences Rd E, University of California, Irvine, CA 92715. Fax: (714) 824-8413.

0090-8258/97 $25.00

sis allows selective diagnosis of cancer if (1) the photosensitizer is preferentially accumulated by the target tissue (e.g., ovarian cancer), and (2) excitation of the photosensitizer with light at the appropriate wavelength results in PpIX fluorescence that can provide contrast between tumor and normal tissue. Although substantial work has been performed in porphyrin sensitizers, such as hematoporphyrin derivatives (HPD), especially in the detection of precancerous and cancerous disease of the colon [9], the unique characteristics of ALA-induced PpIX synthesis for selective detection of tumors *in vivo* is just beginning to be explored [10].

It is our hypothesis that selective ALA-induced PpIX production in intraperitoneal (ip) ovarian cancer micrometastases can be achieved because of a higher intratumoral conversion rate of ALA to PpIX compared to the normal surrounding tissues [11]. Proposed mechanisms for the conversion of ALA to PpIX in tumor tissue include: (1) higher intracellular synthesis capacity of PpIX [12]; (2) decrease of key enzymes in the synthetic heme pathway, like ferrochelatase, which will produce accumulation of converted PpIX [13]; and (3) feedback mechanisms controlling the amount of intracellular PpIX [12]. Consequently, ALA can induce direct photosensitization of tumor cells by selective conversion to PpIX, whereas other photosensitizers localize mainly in the vascular stroma of the tumor [14]. Just as topical application of ALA has proven to be an effective photosensitizer in cancers of the skin, bronchi, and breast [12], it is expected that intraperitoneal ALA administration may lead to a high photosensitizer concentration in ovarian tumor infiltrating the peritoneal and serosal surfaces. This in turn should enhance visualization of ovarian tumors and micrometastases by fluorescence.

In this article, we report the feasibility of using exogenous ALA to detect abdominal ovarian cancer micrometastases smaller than 0.5 mm by *in vivo* PpIX fluorescence in a NuTu-19 epithelial ovarian cancer animal model.

MATERIALS AND METHODS

Animals

Pathogen-free Fischer 344 (F344) female rats (109–155 g) were obtained from Harlan Sprague Dawley, Inc. (Indianapolis, IN) and housed in a pathogen-free animal facility at the University of California, Irvine. They were given commercial basal diet and water *ad libitum.* The experimental protocol (No. 95-1646) for the use of these animals in these studies was approved by the Institutional Laboratory Animal Care and Use Committee at U.C. Irvine.

Epithelial Ovarian Carcinoma Animal Model

Studies were performed utilizing the NuTu-19 epithelial ovarian cancer animal model [15]. NuTu-19 was initiated from a poorly differentiated adenocarcinoma which arose in a female athymic mouse after injection of F344 ovarian surface epithelial cells that spontaneously underwent malignant transformation *in vitro.* When injected into the peritoneal cavity of naive F344 rats, these cells grow in the typical fashion of the most common form of human epithelial ovarian carcinoma (i.e., papillary serous adenocarcinoma). This model closely simulates clinical human ovarian cancer by (a) method of intraperitoneal spread; (b) formation of malignant ascites, and (c) propensity for local metastases and organ invasion (omentum, peritoneum, liver, bowel). After ip injection of 10^6 cells, tumors appear grossly on the omentum and peritoneum (Week 3) as small nodules (0.5 to 2 mm) with the animals exhibiting only minimal ascites (<3 ml). Thereafter, the tumor nodules continuously grow to form a confluent omental mass with eventual development of disseminated intraperitoneal carcinomatosis and massive malignant ascites by the time the animals die (approximately 60 days). NuTu-19 cells are maintained in complete medium consisting of RPMI 1640 (Gibco Life Technologies, Grand Island, NY) with 10% heat-inactivated fetal bovine serum (Gemini Bioproducts, Calabassas, CA) at 37°C and 5% CO_2. The cell line was expanded and cryopreserved in liquid nitrogen (10^7 cells/vial) after testing negative for mycoplasma contamination with a Mycotest kit (Gibco Life Technologies). Each experiment was performed by thawing a vial of cells and expanding them biweekly to generate the appropriate cell number.

For these studies, NuTu-19 cells were harvested with 0.25% trypsin (Gibco Life Technologies), washed twice with Dulbecco's phosphate-buffered saline (PBS, Gibco Life Technologies), counted for cell number and viability using trypsin blue exclusion, and injected ip into F344 rats at a concentration of 10^6 viable cells/ml PBS (10^6 cells per animal). Cell viability of at least 90% was required for experimental use. After allowing 3 weeks for tumor growth, tumor-bearing rats and sham-treated rats (1 ml PBS ip without tumor cells) underwent induction anesthesia with an intramuscular injection of ketamine (13 mg/kg) and xylazine (87 mg/kg). Isoflurane and oxygen were provided during surgery for continuous anesthesia. ALA (100, 50, and 25 mg/kg) was injected ip into groups of 24 rats, respectively. ALA (100 mg/kg) was injected intravenously (iv) in the tail vein of three rats. Just prior to these injections, crystallized 5-aminolevulinic acid hydrochloride (DUSA Pharmaceuticals, Inc., Denville, NJ) was diluted to 40 mg/ml in sterile water and titrated with 10 *N* solution of sodium hydroxide to pH 6.5.

Fluorescence Imaging

In order to closely approximate a clinical laparotomy setting, fluorescence evaluation was performed *in vivo.* The first approach was to acquire fluorescence images in different spectral regions in order to compensate for light distribution

inhomogeneities. Since the level of the signal and the sensitivity of the camera required an acquisition time in the order of a few seconds, motion artifacts introduced by respiratory movements of anesthetized animals and filter changes affected image registration. Therefore, we did not use an imaging system, but instead chose to assess *in vivo* fluorescence subjectively by direct visualization using a fluorescent disk as an internal standard. The fluorescent polymethylmethacrylate disk (diameter 1 cm, thickness 1.5 mm) was embedded with fluorescent dye (DCM, Eastman Kodak, Rochester, NY) with optical density $OD_{460} = 0.025$, presenting an emission spectrum close to PpIX (emission maximum near 600 nm). The *in vivo* tissue fluorescence was defined by comparing the tissue fluorescence level to that of the disk: 0 = no fluorescence; 1 = positive fluorescence but less than the disk (moderate); 2 = equal to or stronger than the disk (strong). *Ex vivo* fluorescence images were subsequently recorded with a slow-scan, thermoelectrically cooled CCD camera. This permits sensitive, high dynamic-range ratio measurements.

Determination of in Vivo Fluorescence

In vivo fluorescence was subjectively determined by direct visualization at different time intervals (1.5, 3, and 6 hr) after ALA was administered at different drug concentrations (100, 50, and 25 mg/kg) and administration routes (ip and iv). With continued anesthesia, and with the rat placed in the supine position, a midline laparotomy incision (xyphoid to pubic symphysis) was made. The abdominal viscera and peritoneum were exposed and fluorescence was induced by application of light from a Model B-100 AP ultraviolet lamp (spectrum: 310–395 nm with main emission line at 366 nm) [UVP, Inc., San Gabriel, CA] positioned approximately 15 cm from the anterior abdominal wall of the animal. Positive fluorescence was observed as lesions exhibiting an orange/red color contrasting with the surrounding tissue. To compare fluorescence between different drug concentrations and time points we utilized the fluorescent polymethylmethacrylate disk as an internal standard.

Determination of ex Vivo Fluorescence

After *in vivo* fluorescence measurements, each animal was euthanized with an intracardiac injection of 0.2 ml Eutha-6 (Western Medical Supply, Arcadia, CA) while still under anesthesia. Tissue samples of the tumor-bearing peritoneum, omentum, and small intestine were excised in order to perform *ex vivo* fluorescence measurements. A slow-scan, thermoelectrically cooled CCD camera Model TE/CCD-576 E/UV (Princeton Instruments, Trenton, NJ) was used to record fluorescence images. Excitation was provided by the 514-nm line of an argon-ion laser coupled to a microlens-terminated optical fiber (64 $\mu W/cm^2$ at the sample). Source distribution and fluorescence images were acquired with 500-nm shortpass and 650-nm (±12.5 nm) bandpass filters (Corion Corporation, Holliston, MA), respectively, using 1-sec acquisition times. Image acquisition, processing, and camera control was performed by a MacIntosh computer with IPLab software (Signal Analytics Corp., Vienna, VA). Tissue fluorescence and light distribution images were recorded sequentially for each sample under identical conditions. Dark-noise images were acquired without the excitation source. Images were corrected for both nonuniform illumination and contributing dark noise using the following formula:

$$\text{Corrected fluorescence image} = \frac{\text{Image (650 nm)} - \text{Dark noise (650 nm)}}{\text{Image (500 nm)} - \text{Dark noise (500 nm)}}$$

On the corrected fluorescence image, the mean fluorescence of the peritoneum, the small intestine, and tumor nodules on the omentum and peritoneum was measured.

Fluorescence Microscopy

Imaging of frozen tissue sections, taken at the time of euthanasia, was performed using the same cooled CCD camera and computer system. However, the camera was coupled to an axiovert 10 epifluorescence microscope (Carl Zeiss, Inc., Thornwood, NY) equipped with a 100-W mercury lamp filtered with a 405-nm (±20 nm) bandpass filter (Omega Engineering, Inc., Stanford, CT), to provide excitation at this wavelength, and using a dichorioc mirror FT 440. The emission wavelength was similarly isolated by a 635-nm (± 27.5) bandpass filter. Exposure times were 2 sec. A shutter (Uniblitz, Model T132, Vincent Associates, Rochester, NY) was used to synchronize the CCD camera with the excitation source.

Statistical Analysis

Differences in fluorescence yield at different time points were analyzed using ANOVA. Statistical significance was taken as $P \leqslant 0.05$. If a significant overall difference was present, multiple comparisons were performed using Fisher's PLSD multiple comparison procedure. Data are presented as means ± 1 SE.

RESULTS

Determination of in Vivo Fluorescence

Figures 1 and 2 are 35-mm photographs of animals after laparotomy showing uv-excited *in vivo* fluorescence of peritoneal (Fig. 1A) and omental (Fig. 2A) ovarian cancer metastases with corresponding conventional light images (Figs. 1B and 2B). As shown in these figures, fluorescent tumor nodules were easily visualized against the normal tissue 3 hr following ip administration of 100 mg/kg ALA

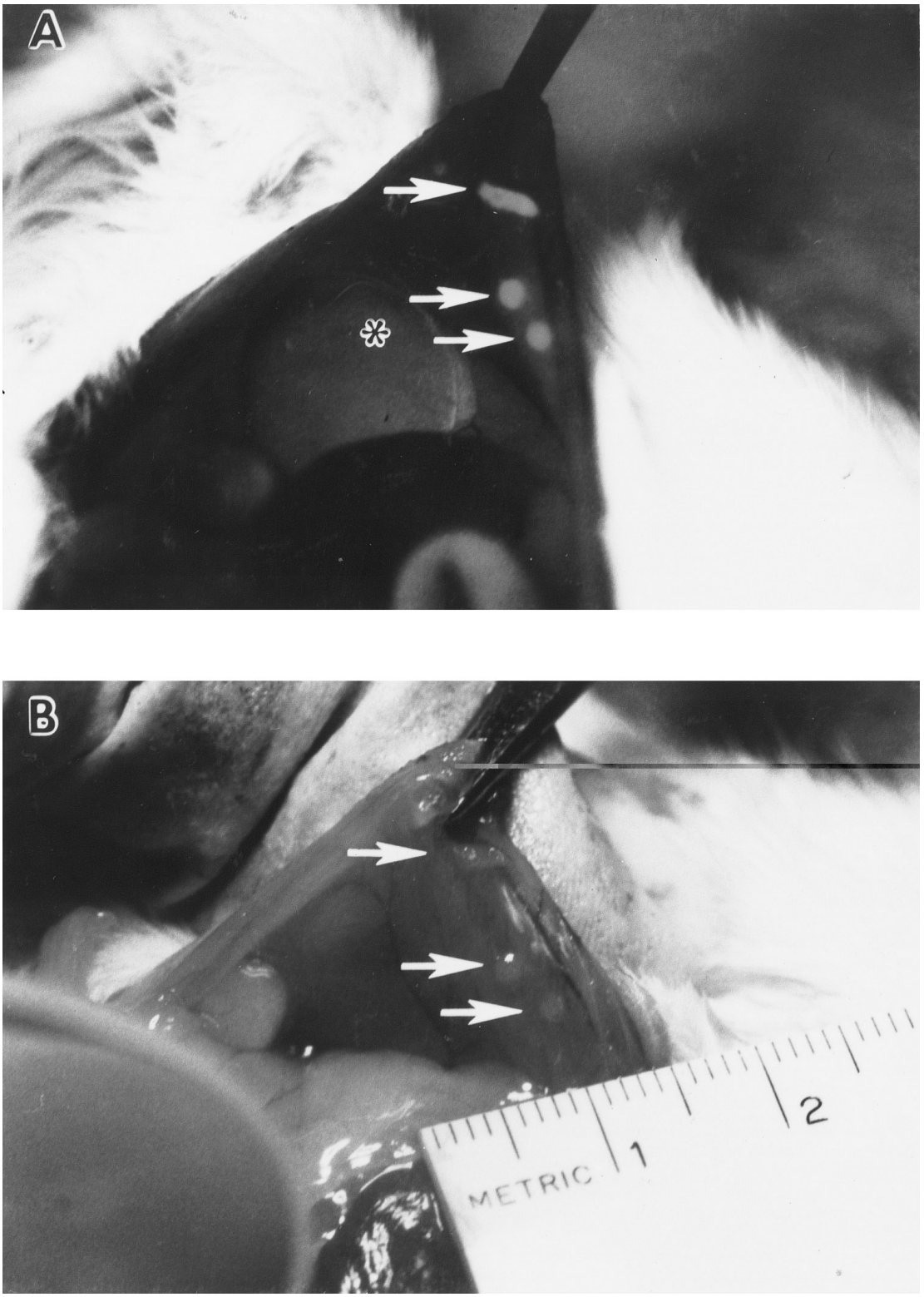

FIG. 1. *In vivo* fluorescence (A) and light images (B) of peritoneal tumor nodules (indicated by arrows). Fluorescence was excited using a uv lamp 3 hr after ip administration of 100 mg/kg ALA. Control fluorescence disk is indicated by an asterisk.

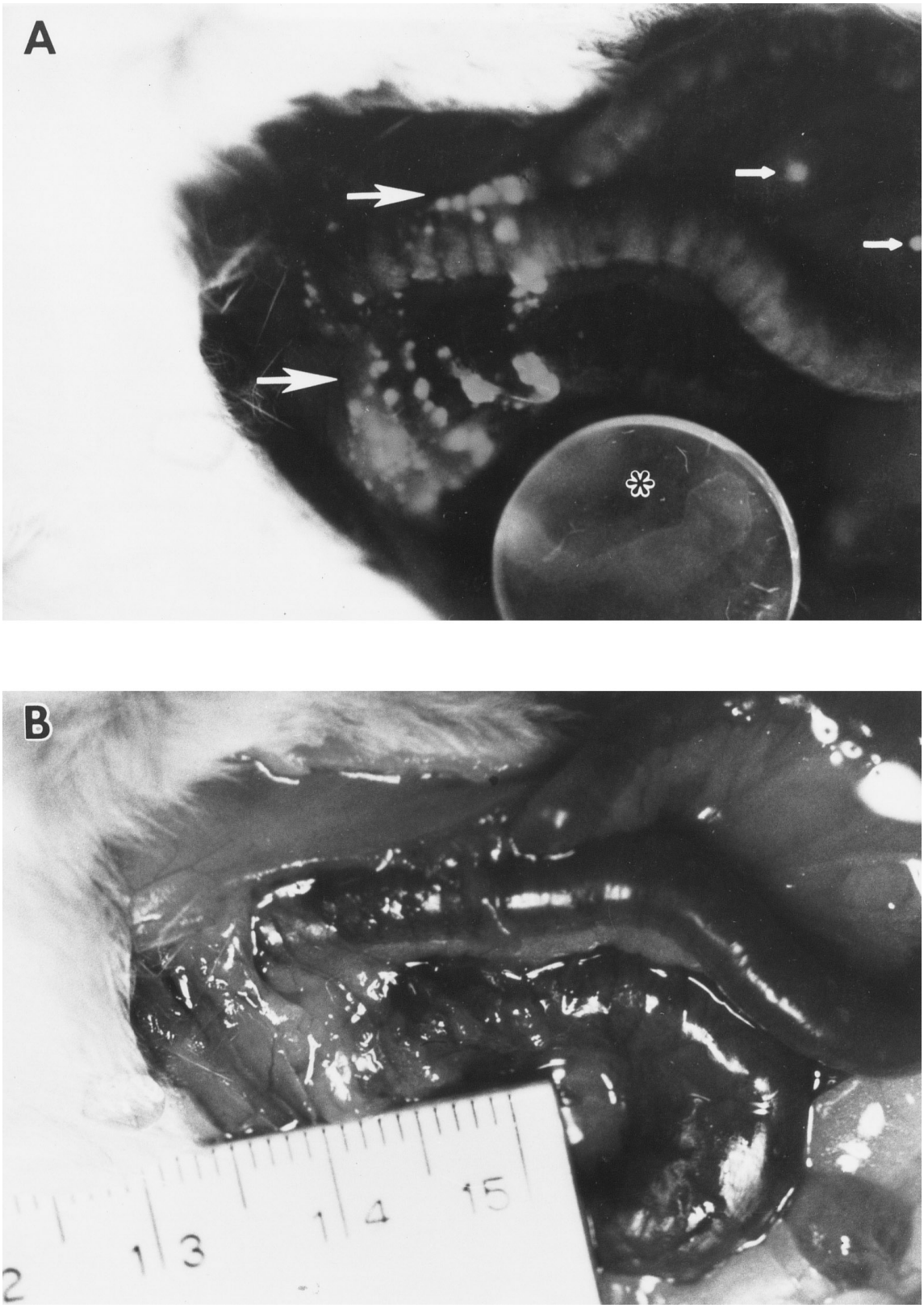

FIG. 2. *In vivo* fluorescence (A) and light images (B) of omental tumor nodules (indicated by large arrows) and small bowel mesentery tumor nodules (small arrows). Transparent omentum is overlying the small bowel. Fluorescence was excited using a uv lamp 3 hr after ip administration of 100 mg/kg ALA. Control fluorescence disk is indicated by an asterisk.

TABLE 1
Number (Percentage) of Animals per Group Showing Strong Red *in Vivo* Fluorescence on Omental and Peritoneal Tumor Nodules

Drug dose in control versus tumor bearing animals	Time after ALA injection (hours)	Number of animals per group	Number (%) of animals with strongly fluorescent omental tumor nodules	Number (%) of animals with strongly fluorescent peritoneal tumor nodules
100 mg/kg (ip) control animals	3 hr post-ALA	5	0 (0%)	0 (0%)
No ALA	0 hr	5	0 (0%)	0 (0%)
100 mg/kg (ip)	1.5 hr post ALA	4	3 (75%)	3 (75%)
100 mg/kg (ip)	3 hr post ALA	9	7 (78%)	6 (67%)
100 mg/kg (ip)	6 hr post ALA	7	5 (71%)	4 (57%)
50 mg/kg (ip)	3 hr post ALA	4	3 (75%)	2 (50%)
25 mg/kg (ip)	3 hr post ALA	4	0 (0%)	0 (0%)
100 mg/kg (iv)	3 hr post ALA	3	2 (66%)	2 (66%)

Note. Strong fluorescence was defined as the tissue having the same or greater levels of fluorescence compared to the fluorescent dye-embedded polymethylmethacrylate disk (grade 2) when irradiated with uv light after ip injection of 100, 50, and 25 mg/kg, and after iv injection of 100 mg/kg ALA in tumor-bearing and control animals.

and excitation with the Woods lamp. Confirmation that the fluorescent nodules were tumor was made by microscopic examination of tissues stained with hematoxylin and eosin (H&E). After ALA application, visible fluorescence of omental and peritoneal tumor nodules was observed in 100% of tumor-bearing animals for all time points, drug concentrations, and both administration routes. Fluorescence could be easily observed in nodules smaller than 0.5 mm. In approximately 70% of tumor-bearing animals, the intensity of fluorescence was strong compared to the control dye disk (grade 2), whereas the remaining 30% showed moderate, but easily visualized fluorescence (grade 1). In contrast, normal tissues adjacent to tumor nodules did not fluoresce (grade 0) and no fluorescence of the tumor nodules could be detected in any animals without administration of ALA. Table 1 summarizes *in vivo* fluorescence evaluation (grading) of omental and peritoneal tumor nodules compared to the fluorescence intensity of the internal standard dye disk. Utilizing a 100 mg/kg ip ALA dose, no significant differences in the percentage of animals exhibiting fluorescence could be seen at 1.5, 3, and 6 hr. Intravenous administration of ALA (100 mg/kg) also did not appear to result in differences in fluorescence intensity or distribution when compared to ip administration. A dose reduction to 50 mg/kg ip showed the same strong tumor fluorescence 3 hr after administration, whereas 25 mg/kg showed a generalized reduced level of fluorescence (grade 1).

Fluorescence and Light Micrographs

Figure 3 shows light micrographs (Fig. 3A) and fluorescence (Fig. 3B) of 5-μm-thick frozen tissue sections 6 hr after administration of ALA at 100 mg/kg ip. A peritoneal tumor nodule (size $<$0.5 mm) and the underlying musculature can be seen. Fluorescence images suggest specific PpIX conversion scattered homogenously throughout the tumor tissue but not in adjacent normal tissue. At the tumor edge it appears that the normal peritoneum is exhibiting ALA-induced fluorescence (boxed area in Fig. 3B). However, microscopic analysis of this region (Fig. 3C) shows a thin layer of infiltrating tumor corresponding with this area of fluorescence. This would suggest a high specificity of the ALA for even small amounts of tumor volume.

Figure 4 shows a cross-sectional view of small bowel in a tumor-bearing animal treated with ip ALA. Strong fluorescence is noted in the intraluminal feces, and immediately adjacent to the mucosal surface lining cells (Fig. 4B). However, the mucosa, submucosa, and muscular layers are without fluorescence. In the cross-sectional images of small bowel from an animal not given ALA (Fig. 5), weak autofluorescence can also be detected in the intraluminal feces (Fig. 5B) in a pattern similar to, but less intense than the pattern seen in the ALA-treated animal (Fig. 4B). Interestingly, fluorescence can be seen on the serosal surface of this ALA-treated tumor bearing animal (Fig. 4B). After examining the tissue under high magnification with H & E staining, this fluorescence was found to be secondary to a superficial layer of NuTu-19 ovarian carcinoma cells.

Determination of ex Vivo Fluorescence

Tumor and peritoneal fluorescence was measured *ex vivo* using the cooled CCD camera. The results shown in Fig. 6 indicate that the tumor fluorescence yield peaks 3 hours after ip ALA administration. The differences in this fluorescence between time points were only significant for the 3-hr time interval (ANOVA, Fisher's PLSD, $P < 0.05$). The ratio between omental tumor nodules and peritoneum was approximately 7 (range 4–10) [data not shown].

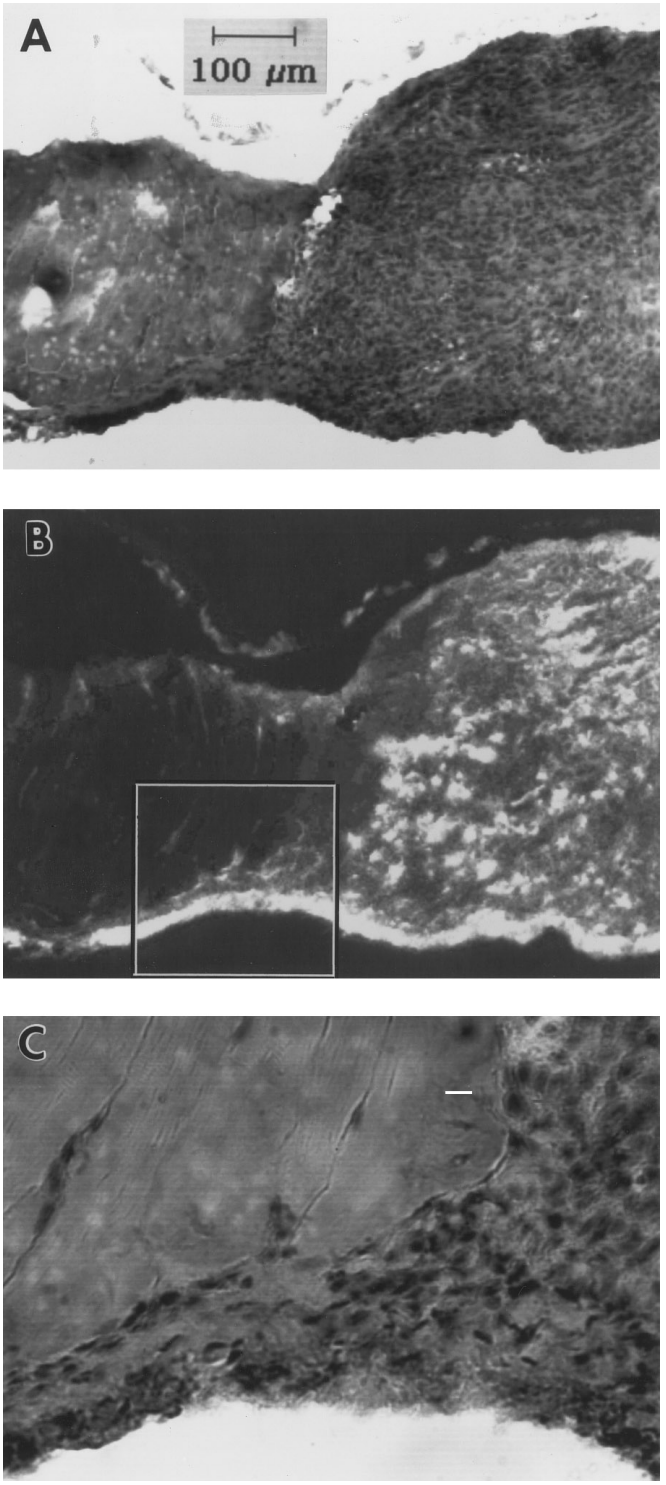

FIG. 3. Light micrographs (A) and fluorescence (B) of a peritoneal nodule (size <0.5 mm) 6 hr after ip ALA administration. Magnification (C) of the peritoneal serosa (boxed area in B) showing a thin layer of tumor matching with the fluorescence.

DISCUSSION

Selective ALA-induced PpIX conversion in ovarian cancers may lead to two new procedures; (1) it may provide an *in vivo* diagnostic aid to improve visualization of micrometastatic ovarian cancer spread in the peritoneal cavity, and (2) it may serve as adjuvant photodynamic therapy for the treatment of micrometastatic (small volume) intraperitoneal disease.

In our study, ALA administration was associated with easily detectable *in vivo* protoporphyrin fluorescence of peritoneal, omental, and serosal micrometastatic ovarian cancer nodules. Strong localized red fluorescence of the ovarian cancer nodules could be observed, compared to the surrounding normal tissue, by illuminating the peritoneal cavity of ALA-treated rats with uv light. The apparent tumor tissue selectivity was likely due to a higher conversion rate of ALA to PpIX by the tumor cells. This observation, in and of itself, is important in that tumor nodules as small as 0.5 mm are extremely difficult to detect by visual means alone. The significance of this finding is that for large surface-area structures, such as the human peritoneal cavity, fluorescence visualization of micrometastatic ovarian cancer implants may enhance our ability to properly stage patients during primary laparotomies or diagnose persistant minimal residual disease during second-look laparotomies. Whereas 100% of the animals exhibited fluorescence of the ovarian cancer nodules after ALA administration, a variation in fluorescence levels was observed (Table 1). This may be due to differences in metabolic rate of ovarian cancer cells, which results in different conversion rate of PpIX or this may be due to quantum yield effects.

What this study did not investigate is the ability to detect retroperitoneal disease; which occurs in 12% of patients with recurrent ovarian cancer after a negative second-look laparotomy [16].

The fluorescence yield at varying time intervals after ALA administration was an interesting finding in this study. PpIX was sufficiently abundant to yield strong fluorescence in as little as 1.5 hr after administration and this fluorescence was still present at 6 hr. This observation is consistent with porphyrin tissue extraction data of carcinoma in tumor-bearing rats, where the decline of tissue porphyrin was observed between 5 and 12 hr after iv ALA administration [11]. As a result of the presented fluorescence data, we postulate that the early fluorescence phase may be secondary to the selective rapid uptake of ALA and its conversion to PpIX in tumor tissue. This early phase is then followed by a second persistent phase of intracellular retention of PpIX. This is supported by the fact that the further metabolism of PpIX is a relatively slow process [12].

The only normal tissue found in this study to exhibit strong *in vivo* fluorescence after ALA administration was the proximal small bowel. Strong fluorescence was visualized in

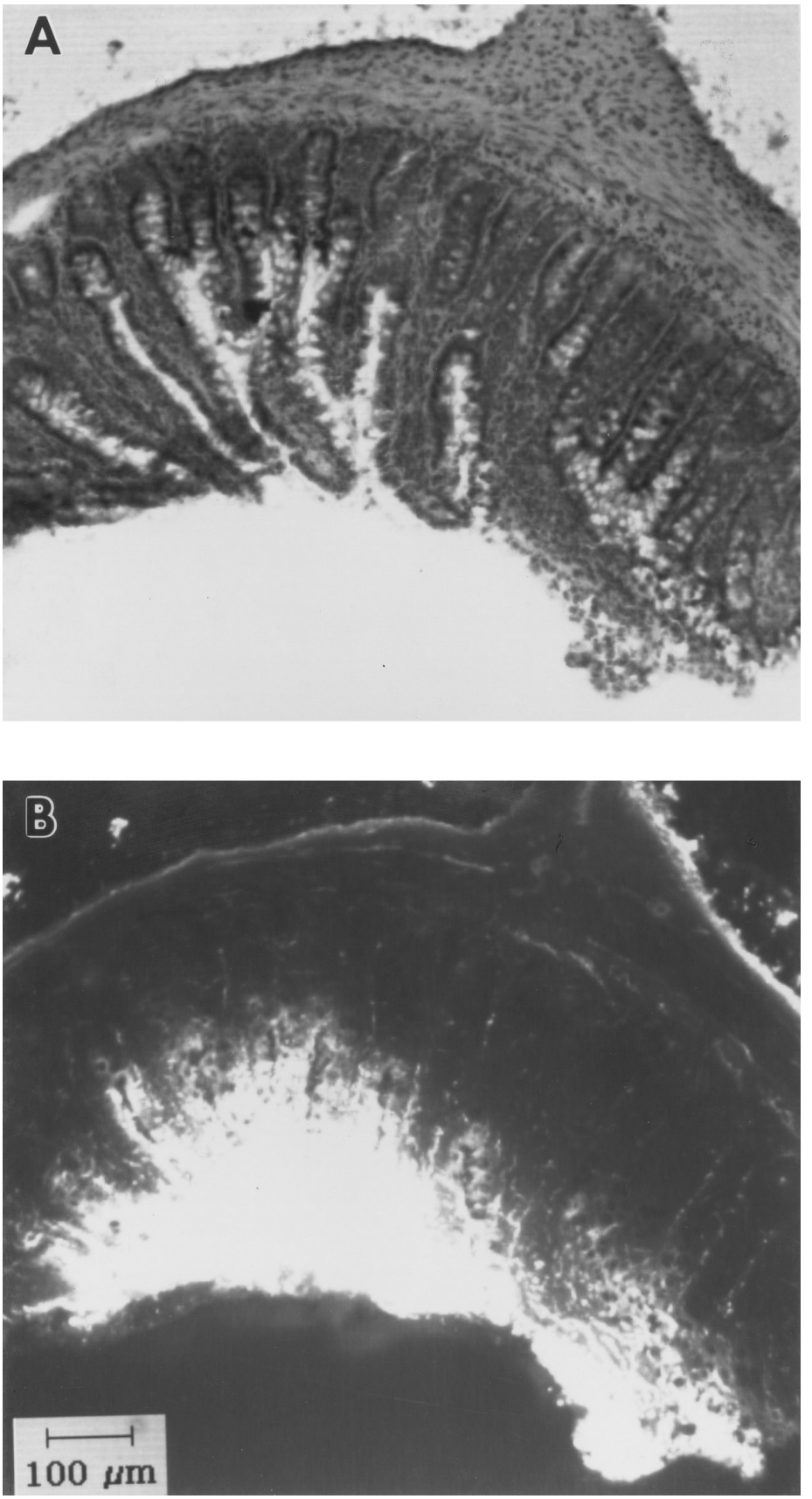

FIG. 4. Light micrographs (A) and fluorescence (B) of small intestine 6 hr after ip ALA.

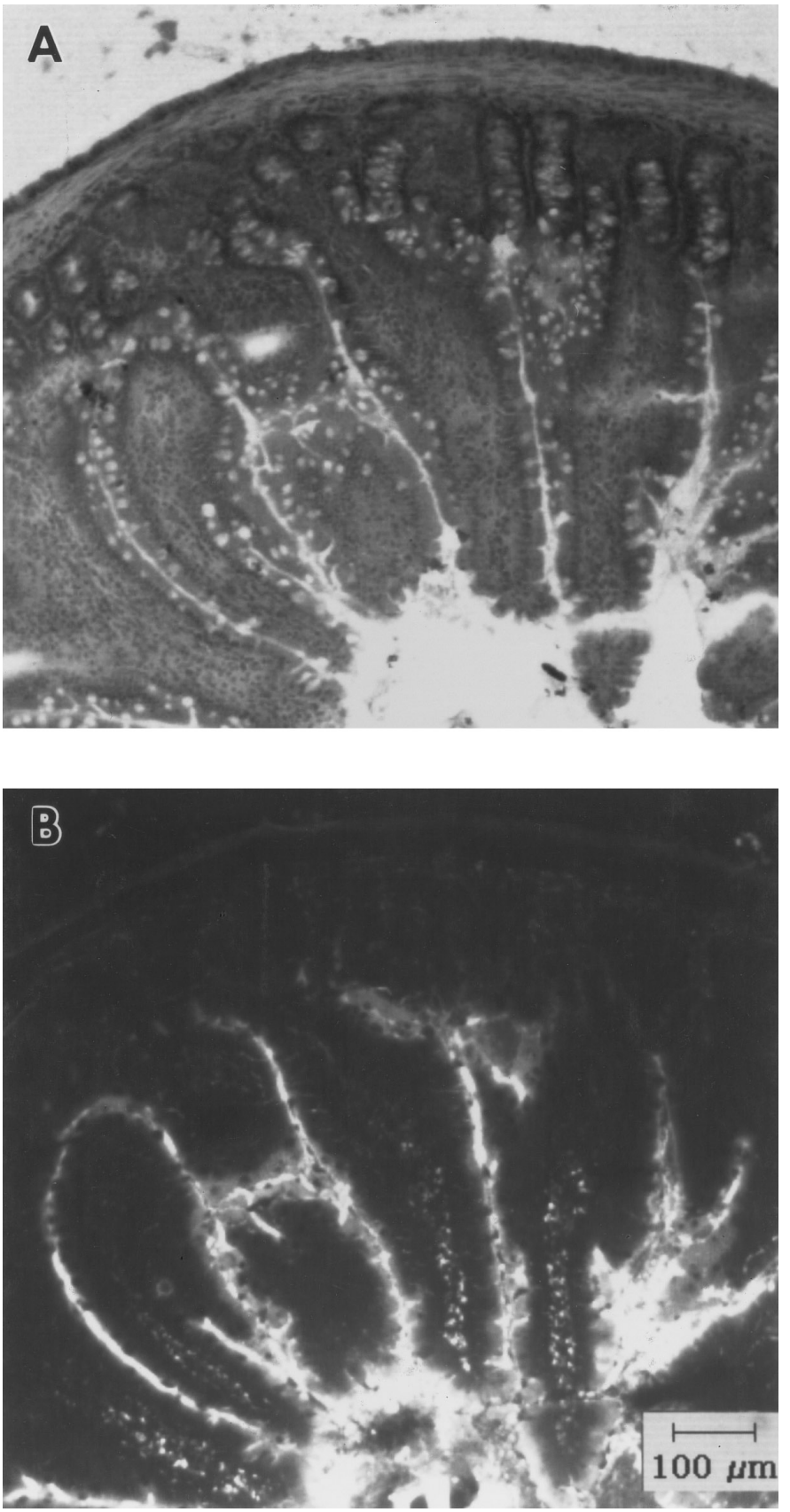

FIG. 5. Light micrographs (A) and autofluorescence (B) of small intestine in an animal not receiving ALA.

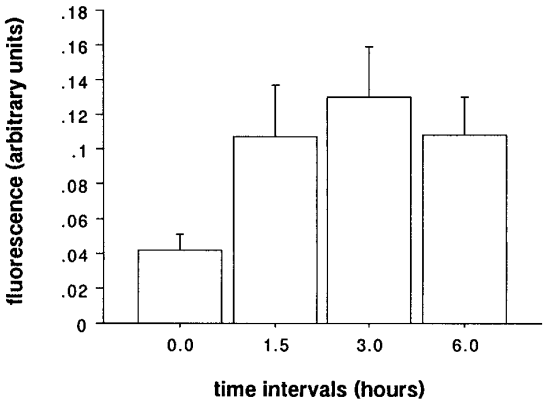

FIG. 6. Fluorescence yield of intraperitoneal tumor nodules. Points represent means ± SE, 4 animals per time interval.

the duodenum and jejunum and feces from the point of entry of the common bile duct to the distal part of the jejunum. Studies on small bowel tissue sections revealed that this fluorescence was due to intraluminal fecal material, and no fluorescence was noted in small bowel mucosa, submucosa, or the muscular layers. These findings could be accounted for by porphyrin excretion in the bile followed by normal bowel motility and by the fluorescent feces which can be visualized through the thin-walled small bowel of the rat. We would expect that the thicker jejunum in humans (approximately 5 mm) would prevent this transluminal visualization of fluorescent fecal material.

In this study, ip application of ALA was comparable to the iv route for *in vivo* fluorescence detection. Because ALA is a small hydrophilic molecule which diffuses easily through tissue, plasma equilibrium occurs quickly. Dose–response studies indicated an optimal dose of 50 mg/kg in that fluorescence was not increased with 100 mg/kg ip at 3 hr, and was weaker with a dosage of 25 mg/kg. This finding has clinical relevance since the ALA dosage (50 mg/kg) utilized in this study has already been shown to be safe in human clinial trials [17–19].

Colonic and oral cancerous lesions have been shown to produce PpIX after ALA application, resulting in (1) selective fluorescence as compared to normal tissue and (2) good response to PDT [14, 17, 18]. In this animal model of epithelial ovarian cancer, selective ALA conversion resulted in high tumor nodule fluorescence compared to the peritoneum (ratio of 5) but not to the small intestine (ratio of 1). However, it should be noted that fluorescence distribution in the small bowel appeared to be limited to intraluminal feces.

The first successful intraabdominal PDT study in animals utilized an hematoporphyrin derivative as a photosensitizer in a murine ascitic tumor model [20]. This same group began the first human clinical trial with disseminated intraperitoneal malignant neoplasms [21, 22]. In these studies, illumination of large surface areas like the peritoneum produced reversible toxicity in multiple organs. However, small bowel perforations were seen in three of these patients. In a rat study utilizing the photosensitizers photofrin or mesotetrahydroxyphenylchlorin (mTHPC), intestinal organs were the most photosensitive intraabdominal structures and intestinal perforation was the most common cause of death after PDT [23]. Therefore, PDT of the peritoneal cavity may be feasible if the intestinal tract can be protected during treatment. In our study presented here, no significant conversion of PpIX occurred in the submucosal and muscular layers of the intestine, as evidenced by minimal fluorescence. Because of this, ALA may have substantialy less intestinal damaging effects compared to previously utilized photosensitizers. Indeed, homogenous distribution of PpIX in tumors was observed, suggesting that photodynamic destruction of these nodules may be successful. The fact that microscopic tumor on the serosal surface of the peritoneum (Fig. 3B) and of the small bowel (Fig. 4B) showed photosensitizer conversion may lead to improvement of adjuvant treatment of intraperitoneal micrometastatic disease.

In summary, as many as 50% of Stage III and Stage IV epithelial ovarian cancer patients who have undergone negative second-look laparotomies will experience subsequent intraabdominal recurrence of their disease [2]. This fact suggests that even a very thorough exploration does not reveal micrometastatic residual disease in many patients. Considering the large surface area of the human peritoneal cavity, increasing the diagnostic efficiency may be best achieved using fluorescence-based visualization techniques. Using this approach we were able to detect tumor nodules as small as 0.5 mm in an experimental animal model. Second-look operations by laparoscopy may significantly benefit from fluorescence detection, in the same way bladder cancer diagnosis was aided by cytoscopy [10]. Additionally, selective and homogenous distribution of PpIX in ovarian cancer tumors predispose ALA as a good candidate for PDT of the peritoneal cavity. In conclusion, specific detection of rat ovarian cancer could be achieved with administration of a nontoxic dose of ALA. This approach may be a promising method for improving the specificity and sensitivity of ovarian cancer tumor staging. In addition, systemic ALA could eventually be coupled with appropriate light delivery and laparoscopic instruments in order to theoretically develop minimally invasive treatment or screening tools for ovarian cancer micrometastases.

ACKNOWLEDGMENTS

This work was supported primarily by NIH Grant ROI CA 322 4 A (M.B.), and in part by grants from Hermann Klaus Foundation, (Zurich, Switzerland) [A.M.], Ciba Geigy Jubilee Foundation, (Basel, Switzerland) [A.M.], Memorial Health Services, Long Beach Memorial Medical Center (Long Beach, CA), the United States Army [S.R.], the Pfeiffer Foundation (S.R., J.H.), and Beckman Laser Institute Programmatic support from ONR Grant N00014-91-C-0134, DOE Grant DE-FG03-91ER61227, and NIH LAMMP Grant RR-01192, Optical Biology resource facilities [B.T., Y.T.,

M.B.]. The authors thank Chung Ho Sun, Lih-Huei L. Liaw, and Sam Choe for excellent technical assistance throughout these studies.

REFERENCES

1. Boring, C. C., Squires, T. S., Tong, T., and Montgomery, S. Cancer statistics, 1994, *Ca Cancer J. Clin.* **44,** 7–26 (1994).
2. DiSaia, P. J., and Creasman, W. T. Epithelial Ovarian Cancer, in *Clinical gynecological oncology* (P. J. DiSaia and W. T. Creasman, Eds.), Mosby-Year Book, St. Louis, pp. 333–425 (1993).
3. Moan, J., and Berg, K. Photochemotherapy of cancer: Experimental research, *Photochem. Photobiol.* **55,** 931–948 (1992).
4. Fisher, A. M., Murphree, A. L., and Gomer, C. J. Clinical and preclinical photodynamic therapy, *Lasers Surg. Med.* **17,** 2–31 (1995).
5. Roberts, W. S., Hodel, K., Rich, W. M., and DiSaia, P. J. Second-look laparotomy in the management of gynecologic malignancy, *Gynecol. Oncol.* **13,** 345–355 (1982).
6. Friedman, J. B., and Weiss, N. S. Second thoughts about second-look laparotomy in advanced ovarian cancer, *N. Engl. J. Med.* **322,** 1079–1082 (1990).
7. Berek, J. S., and Hacker, H. F. Staging and second-look operations in ovarian cancer, in *Ovarian cancer* (D. S. Alberts and E. A. Survit, Eds.), Martinus Nijhoff, Boston, pp. 109–127 (1985).
8. Kennedy, J. C., Pottier, R. H., and Pross, D. C. Photodynamic therapy with endogenous protoporphyrin IX: Basic principles and present clinical experience. *J. Photochem. Photobiol. B* **6,** 143–148 (1990).
9. von Rueden, D., McBrearty, F. X., Clements, B. M., and Woratyla, S. Photo detection of carcinoma of the colon in a rat model: A pilot study. *J. Surg. Oncol.* **53,** 43–46 (1993).
10. Steinbach, P., Kriegmair, M., Baumgartner, R., Hofstadter, F., and Knuchel, R. Intravesical instillation of 5-aminolevulinic acid: The fluorescent metabolite is limited to urothelial cells, *Urology* **44,** 676–681 (1994).
11. Hua, Z., Gibson, S. L., Foster, T. H., and Hilf, R. Effectiveness of delta-aminolevulinic acid-induced protoporphyrin as a photosensitizer for photodynamic therapy in vivo, *Cancer Res.* **55,** 1723–1731 (1995).
12. Kennedy, J. C., and Pottier, R. H. Endogenous protoporphyrin IX, a clinically useful photosensitizer for photodynamic therapy. *J. Photochem. Photobiol. B* **14,** 275–292 (1992).
13. Van Hillegersberg, R., Van den Berg, J. W., Kort, W. J., Terpstra, O. T., and Wilson, J. H. Selective accumulation of endogenously produced porphyrins in a liver metastasis model in rats, *Gastroenterology* **103,** 647–651 (1992).
14. Bedwell, J., MacRobert, A. J., Phillips, D., and Bown, S. G. Fluorescence distribution and photodynamic effect of ALA-induced PP IX in the DMH rat colonic tumour model, *Br. J. Cancer* **65,** 818–824 (1992).
15. Rose, S. G., Tocco, L. M., Granger, G. A., DiSaia, P. J., Hamilton, T. C., Santin, A. D., and Hiserodt, J. C. Development and characterization of a clinically useful animal model of epithelial ovarian cancer in the Fischer 344 rat, *Am. J. Obstet. Gynecol.*, in press (1996).
16. Vaccarello, L., Rubin, S. C., Vlamis, V., Wong, G., Jones, W. B., Lewis, J. L., and Hoskins, W. J. Cytoreductive surgery in ovarian carcinoma patients with a documented previously complete surgical response, *Gynecol. Oncol.* **57,** 61–65 (1995).
17. Grant, W. E., Hopper, C., MacRobert, A. J., Speight, P. M., and Bown, S. G. Photodynamic therapy of oral cancer: Photosensitisation with systemic aminolaevulinic acid, *Lancet* **342,** 147–148 (1993).
18. Loh, C. S., MacRobert, A. J., Bedwell, J., Regula, J., Krasner, N., and Bown, S. G. Oral versus intravenous administration of 5-aminolaevulinic acid for photodynamic therapy, *Br. J. Cancer* **68,** 41–51 (1993).
19. Mlkvy, P., Messmann, H., Regula, J., Conio, M., Pauer, M., Millson, C. E., MacRobert, A. J., and Bown, S. G. Sensitization and photodynamic therapy (PDT) of gastrointestinal tumors with 5-aminolaevulinic acid (ALA) induced protoporphyrin IX (PPIX): A pilot study, *Neoplasma* **42,** 109–113 (1995).
20. Tochner, Z., Mitchell, J. B., Harrington, F. S., Smith, P., Russo, D. T., and Russo, A. Treatment of murine intraperitoneal ovarian ascitic tumor with hematoporphyrin derivative and laser light, *Cancer Res.* **45,** 2983–2987 (1985).
21. Sindelar, W. F., DeLaney, T. F., Tochner, Z., Thomas, G. F., Dachoswki, L. J., Smith, P. D., Friauf, W. S., Cole, J. W., and Glatstein, E. Technique of photodynamic therapy for disseminated intraperitoneal malignant neoplasms. Phase I study, *Arch. Surg.* **126,** 318–324 (1991).
22. DeLaney, T. F., Sindelar, W. F., Tochner, Z., Smith, P. D., Friauf, W. S., Thomas, G., Dachowski, L., Cole, J. W., Steinberg, S. M., and Glatstein, E. Phase I study of debulking surgery and photodynamic therapy for disseminated intraperitoneal tumors, *Int. J. Radiat. Oncol. Biol. Phys.* **25,** 445–457 (1993).
23. Veenhuizen, R. B., Ruevekamp, H. M., Helmerhorst, T. J., Kenemans, P., Mooi, W. J., Marijnissen, J. P., and Stewart, F. A. Intraperitoneal photodynamic therapy in the rat: Comparison of toxicity profiles for photofrin and MTHPC, *Int. J. Cancer* **59,** 830–836 (1994).